Uncovering Scaling Laws to Infer Multi-drug Response of Resistant Microbes and Cancer Cells

Uncovering scaling laws to infer multi-drug response of resistant microbes and cancer cells

Kevin B. Wood[1], Kris C. Wood[2,3], Satoshi Nishida[1], Philippe Cluzel[1,*]

[1]FAS Center for Systems Biology, Department of Molecular and Cellular Biology, School of Engineering and Applied Sciences, Harvard University, 52 Oxford St, Cambridge, MA 02138, USA.

[2] Whitehead Institute for Biomedical Research, 9 Cambridge Center, Cambridge, MA 02142, USA.

[3]Current address: Department of Pharmacology and Cancer Biology, Duke University School of Medicine, Durham, NC 27710, USA.

* To whom correspondence should be addressed: cluzel@mcb.harvard.edu

Drug resistance in bacterial infections and cancers constitutes a major threat to human health. Treatments often include several interacting drugs, but even potent therapies can become ineffective in resistant mutants. Here we simplify the picture of drug resistance by identifying scaling laws that unify the multi-drug responses of drug sensitive and drug resistant cells. Based on these scaling relationships, we are able to infer the two-drug response of resistant mutants in previously unsampled regions of dosage space in clinically relevant microbes such as *E. coli, E. faecalis, S. aureus* and *S. cerevisiae*, as well as in human non-small cell lung cancer, melanoma, and breast cancer stem cells. Importantly, we find that scaling relations also apply across evolutionarily close strains. Finally, scaling allows one to rapidly identify new drug combinations and predict potent dosage regimes for targeting resistant mutants without any prior mechanistic knowledge of the specific resistance mechanism.

Main Text

Introduction

Treatment strategies for infectious diseases and cancers often involve multiple drugs that must be combined, adapted, and refined to target evolving cell populations. Multi-drug therapies can be difficult to design because drugs often interact, making their combined effects larger or smaller than expected from their individual effects (Bliss, 1956; Fitzgerald et al., 2006; Greco et al., 1995; Keith et al., 2005; Lehar et al., 2008; Loewe, 1953). Furthermore, well-developed multi-drug treatments can be thwarted due to the

emergence of multi-drug resistance, which arises in both bacterial infections and cancer and represents a growing public health threat (Levy and Marshall, 2004). For example, potent drug regimens designed to target a particular cancer may be rendered ineffective by the rapid evolution of drug-resistance (Garrett and Arteaga, 2011; Glickman and Sawyers, 2012; Poulikakos and Rosen, 2011). In addition, drugs may interact differently in each new resistant mutant, making the molecular characterization of resistance a time-consuming and at times an untenable goal. Because of the rapidly increasing number of multi-drug resistant mutants, there is significant need for new strategies to characterize and refine drug regimens in hopes of mitigating the effects of resistance.

Scaling laws can offer a complementary approach for simplifying the picture of multi-drug-resistance without relying on highly time- and resource-consuming molecular studies. These laws—which can be surprisingly simple—are often based on symmetry arguments rather than system-specific microscopic details. Scaling is powerful because it offers a quantitative unifying framework for systems that appear, on the surface, to be very different. For example, allometric scaling laws (Shoval et al., 2012) connect anatomical and physiological features, such as body mass and metabolism, across a wide range of organisms. Similar relations have contributed to understanding phenotypic variability in populations of bacteria (Balaban et al., 2004) and eukaryotic immune cells (Feinerman et al., 2008), the fluctuation-response relationship in bacterial chemotaxis (Park et al., 2010), the structural properties of metabolic networks (Jeong et al., 2000), growth and gene expression in populations of *E. coli* (Scott et al., 2010), and epistatic interactions between genes in yeast (Velenich and Gore, 2013). Motivated by the success of scaling laws across disciplines, here we set out to identify similar principles that unify the description of drug interactions in sensitive and resistant cells. The discovery of such scaling relations could provide a new approach for systematically adapting multi-drug treatments to effectively combat drug resistance, even before molecular mechanisms have been fully elucidated.

Results

Drug Interactions Can Change Following Acquisition of Resistance

We first asked how acquired drug resistance affects the interactions between two drugs observed initially in wild-type, drug-sensitive cells. To answer this question, we measured population growth of a wide range of organisms, including bacteria and human cancer cells, in response to drug pairs (Supplemental Information Section I, Tables S1-S3). We then quantified the nature of drug interaction—synergy or antagonism—in both wild type and resistant cells using two standard pharmacology approaches (Figure 1; Figure S1). Interestingly, we find that resistance can alter not only the individual drug efficacies, but also the *interactions* between drugs. That is, two drugs can interact quite differently depending on whether they are applied to drug resistant mutants or drug sensitive cells (Figures 1, S1). For example, the combination of two anti-cancer agents, Gefitinib and 17-AAG, is antagonistic for most dosages in *EGFR*-mutant non-small cell lung cancer (NSCLC) cells, making it an unlikely *a priori* choice for therapy (Figure 1A). However, the same drug pair becomes synergistic for most dosages (Xu et al., 2012) in a Gefitinib-resistant mutant (Engelman et al., 2007) (Figure 1A). On the other hand, in *E. coli*, the antagonism between some drug pairs is eliminated (Figure 1B) or reduced (Figure 1C) in antibiotic-resistant mutants, but the interactions do not become synergistic. A similar decrease in the interactions between antibiotics occurs in vancomycin-resistant *E. faecalis* (Palmer et al., 2011), where the synergy (Rand and Houck, 2004) in the combination of daptomycin and ampicillin is reduced in certain daptomycin-resistant mutants (Figure 1D). By contrast, in *E. coli* exposed to the weakly synergistic combination of doxycycline and erythromycin, the drug pair becomes increasingly synergistic in some multi-drug resistant mutants (Figure 1E). We also observe cases where the drug interactions are not changed by resistance events. For example, the antibiotics chloramphenicol and norfloxacin show approximately the same level of antagonism in *S. aureus* cells and norfloxacin-resistant mutants. In this case, the mutation reduces the effective concentration at which norfloxacin becomes toxic but otherwise does not modify the shape of the cell's two-drug response surface; similar results have been reported for some mutations in *E. coli* (Chait et al., 2007). In summary, we find that resistance can alter drug interactions in multiple different ways, and there is no obvious relationship between the interactions observed in sensitive cells and those in resistant mutants.

A Simple Model Can Describe a Wide Range of Two-Drug Response Surfaces

To establish a relationship between drug interactions before and after the acquisition of resistance, we constructed a simple model to quantitatively characterize growth response surfaces to two drugs. Response surfaces are commonly used for quantifying and classifying the interactions between two drugs based on measurements of cell proliferation (Fitzgerald et al., 2006; Greco et al., 1995; Lehar et al., 2008; Lehar et al., 2007). However, most models apply to only a subset of all measured response surfaces because they are based on simplified enzyme kinetics or are specific to particular drugs classes and particular intracellular pathways (Fitzgerald et al., 2006; Greco et al., 1995; Lehar et al., 2008; Lehar et al., 2007). To account for different types of response surfaces, we used a model of the following multiplicative form,

$$g_{1,2} = g_1(D_1)\, g_2(D_{2eff}), \qquad (1)$$

where $g_{1,2}$ is the growth in the presence of drugs 1 and 2 together, g_1 is the growth as a function of drug 1 alone, and g_2 is the growth as a function of drug 2 alone. D_1 is the concentration of drug 1, and D_{2eff} is the effective concentration of drug 2, which accounts for interactions between the drugs . Changing the concentration D_2 into D_{2eff} formally captures the interaction between the two drugs by allowing the presence of one drug (D_1) to modify the effective concentration, and hence the toxicity, of the other (D_2) according to

$$D_{2eff} = D_2\,(1+C(D_1))^{-1}, \qquad (2)$$

Note that D_{2eff} is equal to the concentration D_2 modified by a factor $(1+C(D_1))^{-1}$ that depends only on D_1. This dependence is governed by the function $C(D_1)$, which we call the 2-drug toxicity function (see Supplemental Information, Section II). The specific definition of this factor is empirical and has been chosen by analogy with simple efflux-mediated drug interactions (Wood and Cluzel, 2012). The function $C(D_1)$ will prove essential for establishing scaling relationships between wild type and mutant cells. Importantly, Equations 1 and 2 allow us to decompose two-drug response surfaces into three simpler, one-dimensional "basis functions": $g_1(D_1)$, $g_2(D_2)$, and $C(D_1)$.

We first verified that this model is sufficiently general to describe, with a minimal number of parameters, all experimentally observed response surfaces. Figure 2A shows a typical example of a response surface, in this case for *E. coli,* in the presence of the antibiotics chloramphenicol and ciprofloxacin (for experimental details, see Supplemental Information Section I). Strongly antagonistic behavior between these drug classes has been linked with a suboptimal ratio of protein to DNA in the cell (Bollenbach et al., 2009). Using the measured two-dimensional response surface, we first extracted the 1-drug toxicity functions (g_1 and g_2) and then determined the 2-drug toxicity function $C(D_1)$ empirically from the data. Specifically, we fit the response surface data using the two latter equations and an empirical parameterization for $C(D_1)$. We select the best parameterization of $C(D_1)$ among a set of 11 possibilities using Akaike Information Criteria, a robust model selection technique (Supplemental Information Section II). Together with equation 1, these three functions (g_1, g_2, and $C(D_1)$) determine the bacterial growth response surface for any concentration of the two drugs (Figure 2, right panel).

The model provides a similarly good description for all the 19 additional drug pairs tested (Supplemental Information Section II, Table S5), spanning a wide range of response surfaces and yielding $C(D_1)$ functions with many different shapes (Figure 2B). In some mechanistically tractable cases, the 2-drug toxicity function is constrained by the intracellular molecular pathways underlying the single-drug and multi-drug responses (Supplemental Information Section III, Figure S2). For example, in the multiple antibiotic resistance (MAR) system, $C(D_1)$ is proportional to the activity of the mar promoter (Figure S2B; (Wood and Cluzel, 2012)). More generally, the model decomposes two-dimensional response surfaces into three simpler, empirical functions that do not require a detailed molecular understanding of the drug interaction or mode of action.

The Decomposition of Response Surfaces into Basis Functions Reveals Scaling Relationships Between Drug Sensitive and Drug Resistant Cells

Next, we exploit the decomposition of response surfaces into basis functions to search for mathematical relationships between the multi-drug responses of drug-sensitive and drug-

resistant cells. We hypothesized that certain properties of the basis functions should be conserved when bacteria become drug-resistant. Specifically, we postulate that the effect of resistance can be: (i) to rescale the concentration of each drug, with the scaling factors $a_1$or a_2 specific to each mutant, and/or (ii) to change the interaction between drugs by rescaling the amplitude of the 2-drug toxicity function $C(D_1)$ (Equation 2) by a single parameter, a_3 (Figure 3). Assumption (i) is consistent with known resistance mechanisms, such as up-regulation of efflux pumps (Wood and Cluzel, 2012), enzymatic degradation, or target modification, which all reduce effective intracellular concentrations of a drug (Chait et al., 2007). Assumption (ii) preserves the shape, but not the magnitude, of the 2-drug toxicity function $C(D_1)$. This assumption stems from the idea that new resistant mutants will not fundamentally redefine the strategies that the parent cell has evolved to cope with the stress of specific drugs. There should exist, therefore, a hidden symmetry unifying the responses of drug-sensitive and drug-resistance cells. Under this assumption, however, the two-drug response surface can still change dramatically—for example, from synergistic to antagonistic—when cells become drug resistant. This change is captured entirely by the scaling factor a_3. The hypotheses (i) and (ii) are further motivated by results in the well-characterized MAR system (Wood and Cluzel, 2012) and by numerical toy models (Supplemental Information section III). If accurate, this model predicts that it is possible to unify the response surfaces of drug sensitive and drug resistant cells through simple scaling relations. Importantly, this scaling approach implies that it may be possible to predict the full two-drug response of resistant mutants from a small number of measurements when the response of drug-sensitive cells is known.

To experimentally test the model, we isolated drug-resistant mutants of *E. coli* by growing wild type cells for 30 to 60 generations in various inhibitory concentrations of chloramphenicol (Cm) and ciprofloxacin (Cip) either together or sequentially (see Supplemental Information Section I for experimental details). The concentrations of Cm and Cip were chosen along a single contour of constant growth to keep the conditions of selection approximately constant for all mutants. We then measured the full response surface and extracted the three basis functions describing the effects of the same two drugs (Cm-Cip) on these mutants (Figures 3A, S3A-B). The collection of responses

represents a broad range of behaviors, with mutants exhibiting a resistance to Cip and Cm that varies by an order of magnitude or more (Figure 3A, top panel). However, Figure 3B (bottom panel) demonstrates that these different behaviors can be unified using one single set of basis functions, common to all mutants, and three scaling parameters (a_1, a_2, and a_3) specific to each mutant, thereby supporting our scaling hypotheses.

Additionally, we found that this scaling approach was valid for a wide range of cells across several domains of life, which includes *E.coli*, *E. faecalis,* and human cancer cells (Figure 3C-E). In some cases, we observed statistically significant (as measured by a_3) small changes in drug interaction, for example, from strongly antagonistic to weakly antagonistic (Figure 3C). In other cases, scaling unifies very different phenotypic behaviors, such as the synergy and additivity of ampicillin and daptomycin in wild-type *E. faecalis* and a daptomycin-resistant (Dap-C) mutant (Figure 3D; See also Figure 1D). Even more surprisingly, scaling laws unify the synergy and antagonism of 17-AAG and Gefitinib found in human non-small cell lung cancer (NSCLC) cells and a Gefitinib-resistant mutant (Figure 3E; see also Figure 1A). Thus, while response surfaces can sometimes change markedly when resistance is acquired, we find that the functional forms of the underlying basis functions are conserved.

These results suggest that the response surfaces of drug-resistant cells are constrained by those of the drug-sensitive wild type cells. If true, one could fully characterize the response surface of a resistant mutant by estimating with only a few measurements the scaling parameters a_1, a_2, and a_3, thus eliminating the need for a labor-intensive sampling of the entire surface. Because this rescaling procedure requires very few measurements, it allows one to infer behavior even in unsampled regions of dosage space (Figure 4, schematic).

Scaling Relations Can Be Used To Rapidly Infer Response Surfaces of Resistant Mutants

To examine if scaling relations can be used to predict response surfaces of resistant mutants, we first focused on three clinically relevant bacterial species: *S. aureus, E. faecalis*, and *E. coli*. For *S. aureus,* we measured the full response surface of wild-type and norfloxacin-resistant cells for the drug combination norfloxacin-chloramphenicol, which is antagonistic in wild-type cells (Figure 5A, left panel; see also Figure 1F). Using only 5 randomly selected data points, we estimated the scaling parameters and used them to infer mutant growth in unsampled regions of dosage space. The scaling parameters reflect slightly increased sensitivity to chloramphenicol (a_1>1) and increased resistance to norfloxacin (a_2<<1). The antagonism between drugs is equal to that in wild type cells (a_3 ~ 1, see also Figure 1F), making this example similar to those previously reported in *E. coli* (Figure S3C, (Chait et al., 2007)).

Next, we compared the responses of a daptomycin-sensitive strain and three daptomycin-resistant strains of *E. faecalis* (Palmer et al., 2011) to combinations of daptomycin and ampicillin (Figures 5B, S4A-B See also Figure 1D). These strains were evolved under daptomycin pressure and represent three distinct evolutionary routes to daptomycin resistance, each with a unique set of genetic mutations (Palmer et al., 2011). Using the wild-type basis functions, we are able to predict the two-drug response for each mutant by estimating the parameters a_1, a_2, and a_3. For the ampicillin-daptomycin combination, all three mutants demonstrate significant resistance to daptomycin ($a_1 < 0.02$), increased sensitivity to ampicillin ($a_2 > 1$), and a drug-drug interaction with slightly ($a_3 = 0.87$, Dap-A mutant) or significantly decreased synergy ($a_3 = 0.05$, Dap-C mutant, Figure 5B; see also Figure 3D). We also accurately inferred response surfaces for combinations of daptomycin and linezolid, an oxazolidinone often used to treat infections of the skin as well as pneumonia (Figure S4C-E).

Finally, we tested the scaling hypothesis for two clinically isolated *E.coli* mutants that share a particularly common mechanism of drug resistance: modification of the drug target (Cohen et al., 1989) (748k.01, Figure S4F-G). Specifically, each strain exhibited resistance to DNA synthesis inhibitors (fluoroquinolones) arising from distinct mutations in the gene (*gyrA*) encoding the target topoisomerase (Cohen et al., 1989). In both cases, the 3-parameter scaling provides an excellent prediction of the response surfaces to

chloramphenicol and ciprofloxacin (Figure S4F-G), and all mutants exhibit little resistance to chloramphenicol ($a_1 \sim 1$), strong resistance to ciprofloxacin ($a_2 < 0.1$), and significantly weaker drug-drug suppression ($a_3 < 1$) than in the wild type. These scaling relationships hold as well for multiple *E. coli* laboratory mutants with evolved resistance to protein synthesis inhibitors, including doxycycline, erythromycin, and chloramphenicol (Figure S4H-K; see also Figure 1B, 1E). We also verified the scaling relations in a cycloheximide-resistant mutant of the budding yeast *S. cerevisiae* (Korolev et al., 2012) exposed to a combination of antifungal agents (Figure S4L).

We next asked whether the scaling hypothesis applies to drug combinations targeting human cancer cells, which possess significantly more genetic complexity and redundancy than microbes. Figure 5C shows the previously discussed Gefitinib/17-AAG combination, where strong antagonism in the parental NSCLC cells is replaced by synergy in the Gefitinib-resistant (GR6) mutant (Engelman et al., 2007). Remarkably, our rescaling approach allows us to predict the mutant response surface for all dosage combinations (see also Figure S4N for the same cells with Gefitinib and Paclitaxel). We find that there is little resistance to 17-AAG ($a_1 \sim 1$) but a significant increase in Gefitinib resistance ($a_2 \ll 1$). In addition, a_3 switched signs from positive to negative, which accounts for the observed phenotypic change from antagonistic interaction in the parental cell line to synergistic interaction in the mutant (recall Figure 1A, Figure 3F). In this case, the synergy arises because 17-AAG inhibits HSP90, which leads to decreased MET protein stability (Xu et al., 2012). The loss of MET, in turn, sensitizes the previously resistant cells to Gefitinib. In terms of our scaling model, the Gefitinib resistance inverts the drug-drug coupling effect of 17-AAG on Gefitinib; rather than lowering the Gefitinib toxicity, as in drug sensitive cells, the presence of 17-AAG raises the effective Gefitinib toxicity in mutant cells. These results again demonstrate that the response surfaces can change markedly following the activation of a resistance event, whereas the functional forms of the basis functions are conserved. From a practical perspective, the scaling approach allowed us to rapidly recognize the strong synergy between 17-AAG and gefitinib in resistant cells (Figure 5C), thereby identifying a potent therapy despite the fact that the drugs are antagonistic in drug-sensitive cells. We also show that the full

response surfaces of RAF inhibitor (PLX4720)-resistant melanoma cells to combinations of antineoplastic drugs can be predicted using the same approach (Figure S4M).

Scaling Relations Can Be Used To Increase Potency of Drug Combination Targeting Cancer Stem Cells

Recent research has also focused on the general drug resistance that appears in cancer stem cells (CSCs), which are believed to underlie the resurgence of many tumors following initial drug treatments (Dick, 2009; Gupta et al., 2009; Reya et al., 2001; Sachlos et al., 2012). Whereas drug-resistant mutants are typically resistant to a small number of specific drugs, CSCs are, in general, more drug resistant than the corresponding cancer cells, and the resistance is not driven by mutations (Dick, 2009; Gupta et al., 2009; Reya et al., 2001; Sachlos et al., 2012). Because of their simultaneous resistance to multiple drugs, CSC's offer an opportunity to test our scaling approach in the context of general drug resistance.

We first directly measured the effects of two anti-cancer drugs, Etoposide and Fluorouracil, on immortalized mammary epithelial (HMLE) cells and on matched HMLE populations enriched for mammary CSCs (Gupta et al., 2009). We found that the effects of the individual drugs vary significantly between cells types, with minimum inhibitory concentrations (MIC's) increased by factors of approximately 8.5 for Etoposide and 4 for 5-FU in CSCs. However, the effects of this general drug resistance become more complicated when the drugs are combined. For example, we found that treating the HMLE cells with Etoposide and 5-FU at concentrations of 0.35 mM and 1.5 mM, respectively, results in growth inhibition of about 50% (full growth surface shown in Figure 5D, left panel). One would naively expect a similar inhibition (50%) of CSC growth when the dosages of each drug are increased to account for increased MICs of the drug individually. However, we measured the inhibitory effects of this naïve combination therapy to be only about 20%, substantially less than expected. Interestingly, our scaling approach can correctly predict this non-intuitive result with only a few measurements (Figure 5D). Furthermore, the scaling relations predict improved therapies. For example, using 8.5 mM of Etoposide alone is correctly predicted to restore growth inhibition to the previous 50% levels (Figure 5D, right panel). In this case, we are also able to decrease the total amount of drug used, compared with the intuitive therapy. Our prediction

quantitatively captures the increased antagonism between 5-FU and Etoposide in CSCs and indicates that scaling relations may be applicable to broadly drug-resistant cancer stem cells.

Overall, we see a wide range of a_3 values from experiments in *E coli, E. faecalis, S. aureus*, *S. cerevisiae* and human cancer cells (Figure S4O), including $a_3<0$ (interaction has changed from antagonistic to synergistic or vice versa), $0<a_3<1$ (interaction has decreased in magnitude), and $a_3>1$ (interaction has increased in magnitude). In all cases, the mutant response is reconstructed by rescaling the wild type basis functions with only three scaling parameters (a_1, a_2, a_3) (Figures 5, S4A-N). Therefore, our scaling hypotheses, which are based on conservation of basis functions, hold for all resistant cells characterized in this study. The scaling also correctly preserves the interaction ($a_3=1$) in a drug-with-itself mock experiment (Figure S5A-D).

Observed Scaling Relationships are Unlikely to Occur By Chance

In view of the smoothness of the typical drug-response surfaces, it is tempting to think that any two surfaces could perhaps be rescaled one into another. Therefore, it is not a priori clear whether the scaling relationships reported here reflect some underlying biological similarity between cellular responses or the scaling relationships are likely to exist between any two-dimensional response surfaces. To explore this question, we developed a null model to quantify the probability of observing our scaling results by chance in a random ensemble of smooth response surfaces (Supplemental Information Section V, Figures S5E-F). This analysis reveals that the reported experimental scaling relationships are unlikely to occur by chance ($p<0.1$ for at least 32 of 42 mutants in the study; Figure S5E). We also find that basis functions from some drug pairs can be rescaled to fit a large number of response surfaces, while basis functions from other drug pairs are highly specific to a given drug combination (Figure S5F). Overall, this analysis suggests that the reported scaling relationships do not hold for arbitrary response surfaces and instead represent an unexpected connection between wild-type and mutant response surfaces. In addition, the scaling approach outperforms standard interpolation methods for predicting growth in unsampled regions of dosage space (Supplemental Information

Section V, Figure S5G-J) and is robust to variations in how the scaling parameters are determined (Supplemental Information Section V, Table S7, Figure S5K).

Scaling Relations Reflect Species-Specific and Drug-Specific Relationships

To further explore the limits of the observed scaling relationships, we asked whether basis functions derived from one specific bacterial type could be rescaled to infer response surfaces in other bacterial species. As a consequence of hypothesis (ii) of the model, it should be possible to use identical basis functions for closely species related because they have most likely evolved similar strategies to cope with chemical stressors. To test this idea, we rescaled the wild-type basis functions measured for *E. coli* (strain k01.48) exposed to chloramphenicol (Cm) and ciprofloxacin (Cip) in an attempt to describe the Cm-Cip response surface in mutants from other bacterial strains. We found that scaled versions of the k01.48 Cm-Cip basis provide an excellent description of drug-resistant mutants from the same strain (Cohen et al., 1989) (k01.48, Figure 6A, red). But using the same basis functions yields increasingly poor predictions for mutants of more distant *E. coli* strains (Figure 6A, blue) as well as for cells of distantly related bacteria (*E. faecalis*, Figure 6A, black; *S. aureus*, Figure 6A, green). Our results suggest that the scaling relationships may apply across species of closely related organisms but, in general, they cannot be used to unify the drug-response of distant species.

Similarly, we asked whether the basis functions describing one drug pair could be rescaled to describe the response surface of a different drug pair. To do so, we used the basis functions from the Cm-Cip response surface (*E. coli* (BW25113)) to rescale the response surfaces from other drug pairs in the same strain (Figure 6B). We found that the basis functions associated with Cm-Cip provide an excellent model for the response to Cm-Ofl, a drug pair with similar modes of action. The same basis also provides a good model for some other drug pairs, such as Cm-Linc and Dox-Ofl, while other drug pairs, including Cm-Tmp and Ery-Tmp, cannot be well described with the Cm-Cip basis. Interestingly, the shapes of some sets of basis functions are similar, especially when drugs have similar modes of action. These basis functions may therefore be used to complement existing strategies (Yeh et al., 2006) for functionally classifying drugs

because our results indicate that they encode drug-specific information (see also Table S6).

Discussion

We have experimentally shown that the two-drug responses of sensitive and resistant cells share common features unified by simple, but general, scaling relations. We have tested these scaling relations using a broad collection drugs, including traditional classes of antibiotics (inhibitors of protein synthesis, DNA synthesis, cell wall synthesis, folic acid synthesis), clinically relevant antibiotics (linezolid and daptomycin), and drugs inducing general stress response (salicylate). We have also used both classic chemotherapy drugs, such as alkylating agents, microtubule inhibitors, and topoisomerase inhibitors, as well as targeted therapies. The predictive power of these scaling relations has been demonstrated in a wide range of mutants exhibiting many resistance mechanisms, including drug efflux-mediated resistance, target modification (e.g. fluoroquinolone-resistant *E.coli*, Figure S4F-G), pathway reactivation (Gefitnib-resistant mutant, Figure 1a, 3e, 5c, and PLX4720-resistant A375, Figure S4M), and de-differentiation (CSC's, Figure 6a, 6b). The scaling relations, analogous to phenomenological laws, are not directly noticeable in two-dimensional response surfaces. However, when the surfaces are decomposed into three basis functions, the underlying symmetry is clear: the shapes of these functions do not change when resistance is acquired. Previous work (Lehar et al., 2007) suggests that interactions between inhibitors of a biochemical network reflect the underlying network topology. In our model, these network properties seem to manifest themselves as 2-drug toxicity functions with specific functional forms (Supplemental Information Section III). Our primary experimental result is that, surprisingly, these shapes are not fundamentally altered when cells become resistant, even when the response surfaces of drug-sensitive and drug-resistant cells differ dramatically.

From a molecular perspective, these scaling properties may arise because resistance is conferred by relatively small genetic changes, and not by any major re-wiring of intracellular networks that govern the global response to drugs. Therefore, the

mutant response is inherently constrained by that of the drug-sensitive parental cells. These scaling relations are evident in genetically similar cells, but they break down when applied across evolutionary distant species. Overall, we found these relationships between drug-sensitive and drug-resistant cells to be robust within many organisms, both prokaryotic and eukaryotic, and within many classes of drugs. Therefore, scaling relationships may reduce the complexity of drug resistance studies by unifying the responses of drug resistant mutants with that of drug-sensitive cells even before specific biochemical mechanisms have been elucidated.

Experimental Procedures

Cell lines, strains, and reagents.

Bacteria

A table of bacterial strains is given in Table S1.

Mammalian Cells

HCC827 parental (WT) and Gefitinib-resistant (GR6) cells, the latter of which were evolved by stepwise selection in increasing concentrations of Gefitnib, were obtained from J. Engelman (Massachusetts General Hospital) and grown in RPMI with 10% fetal bovine serum (FBS) and 1% penicillin/streptomycin. HMLE cells stably expressing lentiviral short hairpin RNAs (shRNA) against GFP (control) and E-Cadherin were obtained from P. Gupta (Whitehead Institute for Biomedical Research) and grown in media consisting of equal parts (1) complete MEGM media (Lonza) and (2) DMEM with 10% fetal bovine serum (FBS) and 1% penicillin/streptomycin (Gupta et al., 2009). A375 parental (WT) cells were obtained from ATCC and grown in RPMI with 10% fetal bovine serum (FBS) and 1% penicillin/streptomycin. PLX4720-resistant A375 cells were engineered by stably overexpressing the kinase C-RAF, which can confer resistance to PLX4720 by overriding B-RAF dependence (Montagut et al., 2008). C-RAF-expressing lentiviruses were produced as previously described (Johannessen et al., 2010; Wood et al., 2012). A375 parental cells were infected at a 1:10 dilution of virus in 6-well plates in the presence of 7.5 μg/ml polybrene and centrifuged at 1200g for 1 hour at 37° C. Twenty-four hours after infection blasticidin (10 μg/ml) was added and cells were

selected for 72 hours, after which blasticidin was removed and growth inhibition assays were performed.

Drugs

Drug solutions were made from solid stocks (Table S2). All antibiotic stock solutions were stored in the dark at -20◦ C in single-use daily aliquots. All drugs were thawed and diluted in sterilized media for experimental use.

Growth Inhibition Assays

<u>*Growth Assay for Bacteria*</u>

We inoculated media (LB for *E. coli*, TSB for *S. aureus*, BHI for *E. faecalis*) from a single colony and grew the cells overnight (12 h at 30°C with shaking at 200 rpm for *E. coli*, *S. aureus*; no shaking for *E. faecalis*). Following overnight growth, stationary phase cells were diluted (~5000 fold for *E. coli, S. aureus*; ~1000 fold for *E. faecalis*) in media. Following the initial dilution, *S. aureus* and *E. faecalis* were grown in drug free media for 1 hour prior to adding drugs and transferring to 96 well plates. We transferred *E. coli* to 96-well plates (round bottom, polystyrene, Corning) immediately following dilution. For each experiment, we set up a two-dimensional matrix of 1 or 2 drug combinations in each of four 96-well plates (165-190 μl media per well). For the remainder of the experiment after the addition of drugs (~10-12 h), cells were grown at 30°C (with shaking at 1000 rpm on four identical vibrating plate shakers for *E. coli*; no shaking for *E. faecalis*). A_{600} (absorbance at 600 nm, proportional to optical density OD) was measured at 15-25 min intervals (with one exception; see below) using a Wallac Victor-2 1420 Multilabel Counter (PerkinElmer) combined with an automated robotic system (Twister II, Caliper Life Sciences) to transfer plates between shakers and the reader. Growth rates in bacteria were determined by fitting background-subtracted growth curves (A_{600} vs. time) in early exponential phase (approximately $0.01 < A_{600} < 0.1$) to an exponential function (MATLAB 7.6.0 curve fitting toolbox, The Mathworks). For *S. aureus* with Nor-Cm (Figure 5), effective exponential growth rates were estimated using background subtracted A_{600} measurements at times t = 2 hours and t = 6 hours; true exponential growth curves are therefore not required for this particular assay, which is instead similar

to traditional viability assays that compare cell number at the end of the experiment (see mammalian growth assays, below). Growth rates were normalized by the growth of cells in the absence of drugs. Error bars, unless otherwise noted, are taken to represent +/- one standard error of the fitted parameter.

Growth assay for Mammalian Cells

Cells were trypsinized, counted, and seeded into 96-well plates at 2,500 cells/well. Twenty-four later, DMSO or concentrated dilutions of indicated drugs (in DMSO) were added to cells (1:1,000 in standard media) to yield the indicated final drug concentrations. Cell viability was measured 4 days after drug addition using the Cell Titer Glo® luminescent viability assay (Promega). Viability was calculated as the percentage of control (untreated cells) after background subtraction. Three replicates were performed for each drug/concentration.

Evolved Drug Resistant Mutants in E. coli and S. aureus

Drug resistant *E. coli* mutants were evolved under conditions in Table S3. *S. aureus* norfloxacin resistant mutants were isolated on TSA (Trypric soy agar, BD) plates containing 4 ug/ml Nor, followed by spreading of overnight culture of Newman strain.

Acknowledgements

We thank S. Levy for providing *E. coli* 748k0.1, 1-748, and 1-748MM strains, M. Gilmore for *E. faecalis* V583, DapA, DapB, and DapC strains, M. Muller for *S. cerevisiae* cylcoheximide resistant strains, J. Engelman for the gefitinib-resistant HCC827 G6 cells, and P. Gupta for the HMLE cells for CSC experiments. We thank S. Cocco, R. Monasson, E. Sontag, and N. Wingreen for helpful discussions, C. Guet, T. Surrey, and D. Brady for helpful suggestions on the manuscript, K. Dave for editorial assistance, and all members of the Cluzel lab for technical guidance and scientific suggestions. The authors are indebted to D. Sabatini in whose laboratory experiments on human cells were performed. This work was supported in part by the National Institutes of Health (NIH) Award P50GM081892-02 to the University of Chicago (to PC and SN)

and by a National Science Foundation Postdoctoral Fellowship 0805462 (K.W.).

Author Contributions

KBW and PC designed research. KBW performed all experiments in *E. coli* and *E. faecalis,* cm-cip experiments in *S. aureus,* and all computational work. KCW designed and performed experiments in human cells. SN isolated nor-resistant *S. aureus* mutants and performed cm-nor experiments. KBW, PC wrote and KCW, SN edited manuscript.

Figure captions

Figure 1: ***Resistance that either alters or conserves interactions between drugs in prokaryotic and eukaryotic cells***

Heat maps quantify the drug interaction and classify it as synergistic or antagonistic across a range of active concentrations for both wild type and mutant cells. To quantify the drug interaction at each point on the response surface, we define the interaction parameter $I = \log_2(g_{12} - g_1 g_2 + 1)$, which is positive (blue) for antagonistic, negative (red) for synergistic interactions (Bollenbach and Kishony, 2011), and 0 when there is no interaction ($g_{12} = g_1 g_2$, consistent with Bliss independence). In addition to modifying the resistance of cells to one or more drugs, resistance events can sometimes modify the interactions between drug pairs. See Figure S1 for an alternative quantification of drug interactions. We note that because mutants in this study are resistant to at least one drug, we must use higher drug concentrations for the mutant cells to obtain growth reduction. However, we estimated the drug interactions over concentration ranges that yield growth reduction in mutant approximately similar to that of wild-type cells (Figure S1). Drug concentrations are given in units of μg/ml unless otherwise noted.

A. Gefitinib resistance in non-small cell lung cancer (NSCLC) cells changes the interaction between 17-AAG and gefitinib from strongly antagonistic (suppressive) to synergistic. Units of [17-AAG] are nM and [gefitinib] are μM.

B. Chloramphenicol resistance in *E. coli* changes the interaction between salicylate and chloramphenicol from strongly antagonistic (suppressive) to additive / weakly synergistic.

C. Chloramphenicol and ciprofloxacin resistance in *E. coli* weakens the strongly antagonistic (suppressive) interaction between chloramphenicol and ciprofloxacin, but does not eliminate the antagonism. Units of [ciprofloxacin] are ng/ml.

D. Daptomycin resistance in *E. faecalis* reduces the strongly synergistic interaction between ampicillin and daptomycin.

E. Erythromycin and doxycycline resistance in *E. coli* increases the synergistic interaction between the two drugs.

F. Norfloxacin resistance in *S. aureus* does not change the interaction between chloramphenicol and norfloxacin.

Figure 2: ***Characterization of bacterial response to a pair of drugs using a set of three unique basis functions.***

A. Experimental heat map of growth rate relative to that of untreated cells in response to a pair of drugs (chloramphenicol, Cm, and ciprofloxacin, Cip, left). Red is maximum growth, blue is no growth. See Supplemental Information Section I for estimate of uncertainty in growth rate. [Cm] units are μg/ml, [Cip] units are ng/ml. See related Figure S2.

Drug 1 toxicity (middle top), drug 2 toxicity (middle center), and 2-drug toxicity function ($C(D_1)$, middle bottom). The 1-drug toxicity functions are modelled using the Hill form common in pharmacology, with K_i the concentration of drug i (for i=1,2) at which the effect is half maximal (also known as the IC_{50}), and n_i the Hill coefficient describing the slope of the response. The function $C(D_1)$ is an empirically determined

function that captures the effect of drug 1 (chloramphenicol) on drug 2 (ciprofloxacin) (Equation 2). It is fit directly from data and has the following intuitive interpretation: $C(D_1)=0$ when drug 1 does not alter the effect of drug 2, while $C(D_1)>0$ indicates antagonistic interaction and $C(D_1)<0$ indicates a synergistic interaction. The 1-drug toxicity functions along with $C(D_1)$ accurately describe the entire two-dimensional response surface (right). Circles: experimental measurements; solid lines: nonlinear fits to functional forms in A; error bars: +/- one standard error of the growth rate estimate (Supplemental Information, Section II). The responses to all 19 drug pairs tested are well described by unidirectional 2-drug toxicity functions (Table S5, Figure S2).

B. Example two drug toxicity functions C(D) for six different drug pairs. For example, "C(D) for Tmp" (first panel) describes the effects of chloramphenicol on trimethoprim (Tmp). Concentrations are measured in units of minimum inhibitory concentration (MIC) = K_i for each drug. Ofl, ofloxacin; Tet, tetracycline; Ery, erythromycin.

Figure 3: ***Single drug toxicity functions and coupling functions ($D_{2,eff}/D_2$) for drug-resistant mutants can be rescaled to match those in parental E. coli, E. faecalis, and non-small cell lung cancer (NSCLC) cells.***

A. Single drug toxicity functions (top left, top center) and two drug toxicity functions (top right) for 18 mutant strains isolated by selection in chloramphenicol (Cm) and ciprofloxacin (Cip) at various doses (Table S3, Figure S3). Each color / marker combination represents a single mutant. Drug concentrations are in units of μg/ml for chloramphenicol (323 g/mol) and ng/ml for ciprofloxacin (331 g/mol). C(D) functions are constructed point-by-point from raw growth data (Supplemental Information, Section II).

B. 1-drug toxicity functions (bottom left, bottom center) and 2-drug toxicity functions (bottom right) for all mutant strains are simple re-scalings of the corresponding functions in the wild type cells (Supplemental Information, Section II). A set of three scaling

parameters, (a_1, a_2, a_3), provide a set of coordinates that define each mutant. Specifically, mutant 1-drug and 2-drug toxicity functions are obtained from those of wild type cells by applying the following transformations

$$D_1 \rightarrow D_1' = a_1 D_1$$
$$D_2 \rightarrow D_2' = a_2 D_2$$
$$C \rightarrow C' = a_3 C$$

where a_1, a_2, and a_3 are scaling parameters describing the change in resistance to drug 1, the change in resistance to drug 2, and the change in the amplitude of $C(D_1)$, respectively, in the resistant mutant. Solid line, bottom panels: single toxicity functions (left and center panel) and two drug toxicity function (right panel) that best describe rescaled data.

C.-E. Examples of rescaling the amplitude of $C(D_1)$ to demonstrate the scaling relations in drug-sensitive and drug-resistant cells. Left panels: $C(D_1)$ functions for wild-type (filled circles) and drug-resistant (open circles) cells. Right panels: $C(D_1)$ functions for wild-type (filled circles) and drug-resistant (open circles) cells following a rescaling of the amplitude by a_3. Panel D shows rescaling of WT 2-drug toxicity (black) Dap C mutant (Table S1). Drug concentrations are in units of μg/ml for chloramphenicol (323 g/mol), dapatomycin (1619 g/mol), and ampicillin (349 g/mol), ng/ml for ciprofloxacin (331 g/mol), μM for gefitinib (446 g/mol), and nM for 17-AAG (586 g/mol).

Figure 4: ***Method for inferring response surfaces of drug-resistant mutants from response surfaces of wild type cells.***

The two-drug response surfaces of wild-type (drug sensitive) cells can be used to infer the responses of drug resistant mutants. First, one must extract the 3 basis functions describing the wild type surface (Figure 2). Second, one can estimate the scaling parameters a_1, a_2, and a_3 using a small number of measurements of the mutant response (left) and then fully reconstruct the response surfaces for each mutant (right).

Figure 5: ***Rescaling parameters predict the response of resistant mutants to drug combinations in unsampled regions of dosage space.***

Predicting of the response of resistant mutants to a two-drug combination requires estimation of only three scaling parameters if the wild-type two-drug response is known. (see Figure 4). The responses of resistant mutants to each of three two-drug combinations (chloramphenicol-norfloxacin in *S. aureus* (**A**), ampicillin-daptomycin in *E. faecalis* (**B**), and gefitinib and 17-AAG in NSCLC cells (HCC827) (**C**) are predicted using scaling parameters estimated using the wild-type basis functions and 5 randomly selected measurements of the mutant's growth rate. Similarly, the responses of drug resistant cancer stem cells to etoposide and 5-FU are predicted using scaling parameters estimated using the basis functions from parental cells and 5 randomly selected measurements of the mutant's growth rate. The parameters (a_1, a_2, a_3) describing the mutants, along with standard errors, are given by **A.** (1.37±0.03, 0.10±0.002) (a_3 not needed); **B**. (0.88±0.02, 0.017±0.0005, 0.53±0.06); **C.** (a_1, a_2, a_3) = (0.9±0.05, 0.0043±0.0002, -0.22±0.02). Left panels: heat map of relative growth rate in wild type cells and relative growth rates for 5 randomly chosen dosages in the mutant cells. Right panel, large figure: comparison of experiment and prediction for each drug dosage in the mutant cells. Error bars: +/- standard error of prediction. Inset: Histograms of root mean squared error (RMSE) of the predicted two-dimensional mutant growth surfaces constructed from 2500 independent trials. In each trial, the entire mutant growth surface is predicted using five randomly selected data points on the mutant two-drug surface. Right panels: heat maps of relative growth rate for mutant from experiment (top) and prediction (bottom). Black lines show a single contour of constant growth estimated by smoothing the growth surface using cubic spline interpolation (csaps function in Matlab). Different contour shapes in wild type and mutant cells (panels B, C and D) illustrate that drug interactions have changed (see also Figures 1, S1). Drug concentrations are μg/ml for all drugs except 17-AAG (nM), gefitinib (μM), Etoposide (μM), and 5-FU (μM). See also related Figure S4.

Figure 6: Scaling relations hold across related species or drug classes

A. The basis functions for chloramphenicol (Cm) and ciprofloxacin (Cip) in drug-sensitive *E.coli* (k01.48) are rescaled to fit Cm-Cip response surfaces measured in drug-resistant mutants from the same strain (red) as well as mutants from *E.coli* BW25113 (blue), *E. faecalis* (black), and *S. aureus* (green). Deviation from perfect model is defined as 1- R^2, where the coefficient of determination, R^2, is defined as $R^2 = 1\text{-}SS_{err} / SS_{tot}$ with SS_{err} the residual sum of squares between model and data and SS_{tot} the total sum of squares (proportional to the variance of the experimental measurements. Schematic phylogenetic tree is plotted below the horizontal axis.

B. The basis functions for chloramphenicol (Cm) and ciprofloxacin (Cip) in drug-sensitive *E.coli* (BW25113) are rescaled to fit response surfaces to other drug pairs in the same strain. Deviation from perfect model is defined as in A.

See also Figure S5 for more detailed statistical analysis.

References

Balaban, N.Q., Merrin, J., Chait, R., Kowalik, L., and Leibler, S. (2004). Bacterial persistence as a phenotypic switch. Science *305*, 1622-1625.
Bliss, C.I. (1956). The calculation of microbial assays. Bacteriol Rev *20*, 243-258.
Bollenbach, T., and Kishony, R. (2011). Resolution of gene regulatory conflicts caused by combinations of antibiotics. Mol Cell *42*, 413-425.
Bollenbach, T., Quan, S., Chait, R., and Kishony, R. (2009). Nonoptimal microbial response to antibiotics underlies suppressive drug interactions. Cell *139*, 707-718.
Chait, R., Craney, A., and Kishony, R. (2007). Antibiotic interactions that select against resistance. Nature *446*, 668-671.
Cohen, S.P., McMurry, L.M., Hooper, D.C., Wolfson, J.S., and Levy, S.B. (1989). Cross-resistance to fluoroquinolones in multiple-antibiotic-resistant (Mar) Escherichia coli selected by tetracycline or chloramphenicol: decreased drug accumulation associated with membrane changes in addition to OmpF reduction. Antimicrobial agents and chemotherapy *33*, 1318-1325.
Dick, J.E. (2009). Looking ahead in cancer stem cell research. Nat Biotechnol *27*, 44-46.

Engelman, J.A., Zejnullahu, K., Mitsudomi, T., Song, Y., Hyland, C., Park, J.O., Lindeman, N., Gale, C.M., Zhao, X., Christensen, J.*, et al.* (2007). MET amplification leads to gefitinib resistance in lung cancer by activating ERBB3 signaling. Science *316*, 1039-1043.
Feinerman, O., Veiga, J., Dorfman, J.R., Germain, R.N., and Altan-Bonnet, G. (2008). Variability and robustness in T cell activation from regulated heterogeneity in protein levels. Science *321*, 1081-1084.
Fitzgerald, J.B., Schoeberl, B., Nielsen, U.B., and Sorger, P.K. (2006). Systems biology and combination therapy in the quest for clinical efficacy. Nat Chem Biol *2*, 458-466.
Garrett, J.T., and Arteaga, C.L. (2011). Resistance to HER2-directed antibodies and tyrosine kinase inhibitors. Cancer Biology & Therapy *11*, 793-800.
Glickman, M.S., and Sawyers, C.L. (2012). Converting Cancer Therapies into Cures: Lessons from Infectious Diseases. Cell *148*, 1089-1098.
Greco, W.R., Bravo, G., and Parsons, J.C. (1995). The search for synergy: a critical review from a response surface perspective. Pharmacol Rev *47*, 331-385.
Gupta, P.B., Onder, T.T., Jiang, G., Tao, K., Kuperwasser, C., Weinberg, R.A., and Lander, E.S. (2009). Identification of selective inhibitors of cancer stem cells by high-throughput screening. Cell *138*, 645-659.
Jeong, H., Tombor, B., Albert, R., Oltvai, Z.N., and Barabasi, A.L. (2000). The large-scale organization of metabolic networks. Nature *407*, 651-654.
Johannessen, C.M., Boehm, J.S., Kim, S.Y., Thomas, S.R., Wardwell, L., Johnson, L.A., Emery, C.M., Stransky, N., Cogdill, A.P., Barretina, J.*, et al.* (2010). COT drives resistance to RAF inhibition through MAP kinase pathway reactivation. Nature *468*, 968-U370.
Keith, C.T., Borisy, A.A., and Stockwell, B.R. (2005). Multicomponent therapeutics for networked systems. Nat Rev Drug Discov *4*, 71-78.
Korolev, K.S., Muller, M.J., Karahan, N., Murray, A.W., Hallatschek, O., and Nelson, D.R. (2012). Selective sweeps in growing microbial colonies. Phys Biol *9*, 026008.
Lehar, J., Stockwell, B.R., Giaever, G., and Nislow, C. (2008). Combination chemical genetics. Nature chemical biology *4*, 674-681.
Lehar, J., Zimmermann, G.R., Krueger, A.S., Molnar, R.A., Ledell, J.T., Heilbut, A.M., Short, G.F., 3rd, Giusti, L.C., Nolan, G.P., Magid, O.A.*, et al.* (2007). Chemical combination effects predict connectivity in biological systems. Molecular systems biology *3*, 80.
Levy, S.B., and Marshall, B. (2004). Antibacterial resistance worldwide: causes, challenges and responses. Nat Med *10*, S122-129.
Loewe, S. (1953). The problem of synergism and antagonism of combined drugs. Arzneimittelforschung *3*, 285-290.
Montagut, C., Sharma, S.V., Shioda, T., McDermott, U., Ulman, M., Ulkus, L.E., Dias-Santagata, D., Stubbs, H., Lee, D.Y., Singh, A.*, et al.* (2008). Elevated CRAF as a potential mechanism of acquired resistance to BRAF inhibition in melanoma. Cancer Research *68*, 4853-4861.
Palmer, K.L., Daniel, A., Hardy, C., Silverman, J., and Gilmore, M.S. (2011). Genetic basis for daptomycin resistance in enterococci. Antimicrobial agents and chemotherapy *55*, 3345-3356.

Park, H., Pontius, W., Guet, C.C., Marko, J.F., Emonet, T., and Cluzel, P. (2010). Interdependence of behavioural variability and response to small stimuli in bacteria. Nature *468*, 819-823.
Poulikakos, P.I., and Rosen, N. (2011). Mutant BRAF Melanomas-Dependence and Resistance. Cancer Cell *19*, 11-15.
Rand, K.H., and Houck, H. (2004). Daptomycin synergy with rifampicin and ampicillin against vancomycin-resistant enterococci. The Journal of antimicrobial chemotherapy *53*, 530-532.
Reya, T., Morrison, S.J., Clarke, M.F., and Weissman, I.L. (2001). Stem cells, cancer, and cancer stem cells. Nature *414*, 105-111.
Sachlos, E., Risueno, R.M., Laronde, S., Shapovalova, Z., Lee, J.H., Russell, J., Malig, M., McNicol, J.D., Fiebig-Comyn, A., Graham, M.*, et al.* (2012). Identification of drugs including a dopamine receptor antagonist that selectively target cancer stem cells. Cell *149*, 1284-1297.
Scott, M., Gunderson, C.W., Mateescu, E.M., Zhang, Z., and Hwa, T. (2010). Interdependence of cell growth and gene expression: origins and consequences. Science *330*, 1099-1102.
Shoval, O., Sheftel, H., Shinar, G., Hart, Y., Ramote, O., Mayo, A., Dekel, E., Kavanagh, K., and Alon, U. (2012). Evolutionary Trade-Offs, Pareto Optimality, and the Geometry of Phenotype Space. Science *336*, 1157-1160.
Velenich, A., and Gore, J. (2013). The strength of genetic interactions scales weakly with the mutational effects. Genome Biology (in press).
Wood, K., and Cluzel, P. (2012). Trade-offs between drug toxicity and benefit in the multi-antibiotic resistance system underlie optimal growth of E. coli. BMC Syst Biol *6*, 48.
Wood, K.C., Konieczkowski, D.J., Johannessen, C.M., Boehm, J.S., Tamayo, P., Botvinnik, O.B., Mesirov, J.P., Hahn, W.C., Root, D.E., Garraway, L.A.*, et al.* (2012). MicroSCALE screening reveals genetic modifiers of therapeutic response in melanoma. Science Signaling *5*, rs4.
Xu, L., Kikuchi, E., Xu, C., Ebi, H., Ercan, D., Cheng, K.A., Padera, R., Engelman, J.A., Janne, P.A., Shapiro, G.I.*, et al.* (2012). Combined EGFR/MET or EGFR/HSP90 inhibition is effective in the treatment of lung cancers codriven by mutant EGFR containing T790M and MET. Cancer research *72*, 3302-3311.
Yeh, P., Tschumi, A.I., and Kishony, R. (2006). Functional classification of drugs by properties of their pairwise interactions. Nat Genet *38*, 489-494.

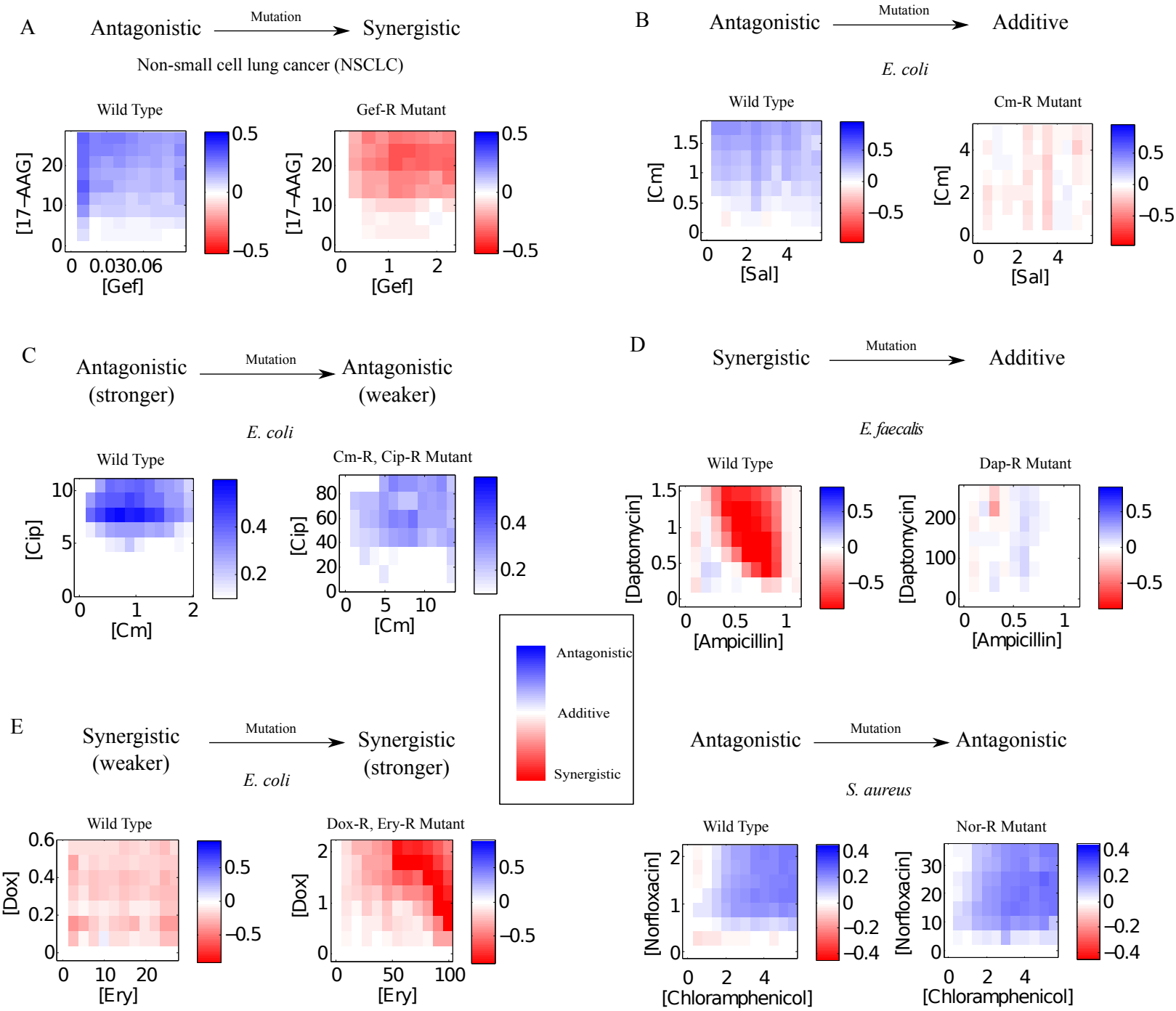
A
Antagonistic
Mutation
Synergistic
Non-small cell lung cancer (NSCLC)
Wild Type
Gef-R Mutant
[17–AAG]
[Gef]
B
Antagonistic
Mutation
Additive
E. coli
Wild Type
Cm-R Mutant
[Cm]
[Sal]
C
Antagonistic (stronger)
Mutation
Antagonistic (weaker)
E. coli
Wild Type
Cm-R, Cip-R Mutant
[Cip]
[Cm]
D
Synergistic
Mutation
Additive
E. faecalis
Wild Type
Dap-R Mutant
[Daptomycin]
[Ampicillin]
Antagonistic
Additive
Synergistic
E
Synergistic (weaker)
Mutation
Synergistic (stronger)
E. coli
Wild Type
Dox-R, Ery-R Mutant
[Dox]
[Ery]
Antagonistic
Mutation
Antagonistic
S. aureus
Wild Type
Nor-R Mutant
[Norfloxacin]
[Chloramphenicol]

Figure 1

A

Figure 2

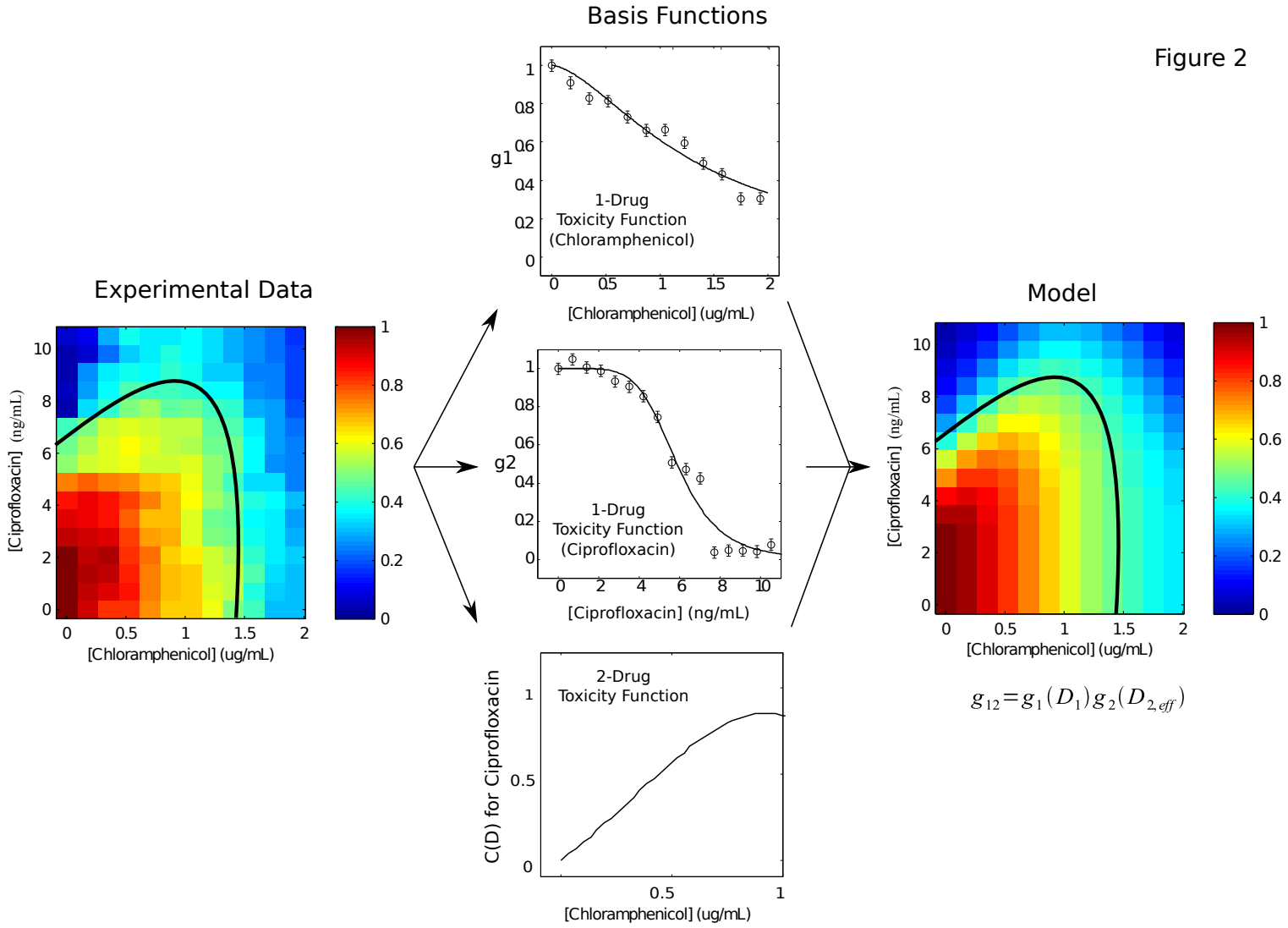

B

Example 2-Drug Toxicity Functions in *E. coli*

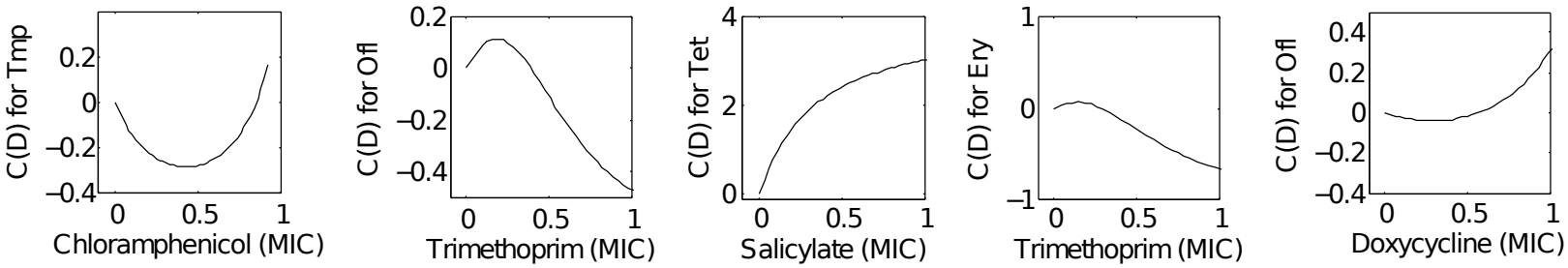

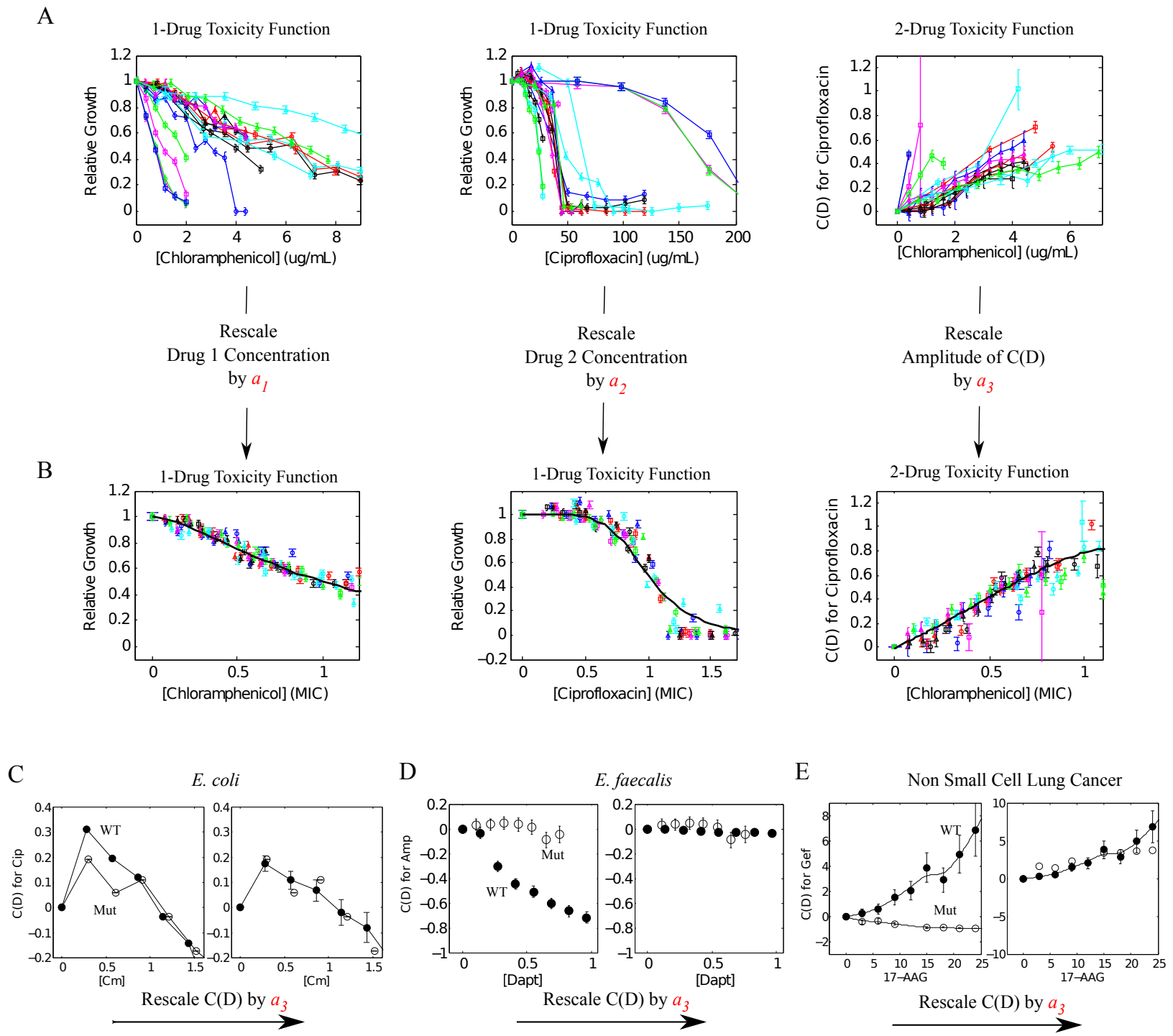
A
1-Drug Toxicity Function
Relative Growth
[Chloramphenicol] (ug/mL)
1-Drug Toxicity Function
Relative Growth
[Ciprofloxacin] (ug/mL)
2-Drug Toxicity Function
C(D) for Ciprofloxacin
[Chloramphenicol] (ug/mL)
Rescale
Drug 1 Concentration
by a_1
Rescale
Drug 2 Concentration
by a_2
Rescale
Amplitude of C(D)
by a_3
B
1-Drug Toxicity Function
Relative Growth
[Chloramphenicol] (MIC)
1-Drug Toxicity Function
Relative Growth
[Ciprofloxacin] (MIC)
2-Drug Toxicity Function
C(D) for Ciprofloxacin
[Chloramphenicol] (MIC)
C
E. coli
C(D) for Cip
WT
Mut
[Cm]
[Cm]
Rescale C(D) by a_3
D
E. faecalis
C(D) for Amp
Mut
WT
[Dapt]
[Dapt]
Rescale C(D) by a_3
E
Non Small Cell Lung Cancer
C(D) for Gef
WT
Mut
17–AAG
17–AAG
Rescale C(D) by a_3

Figure 3

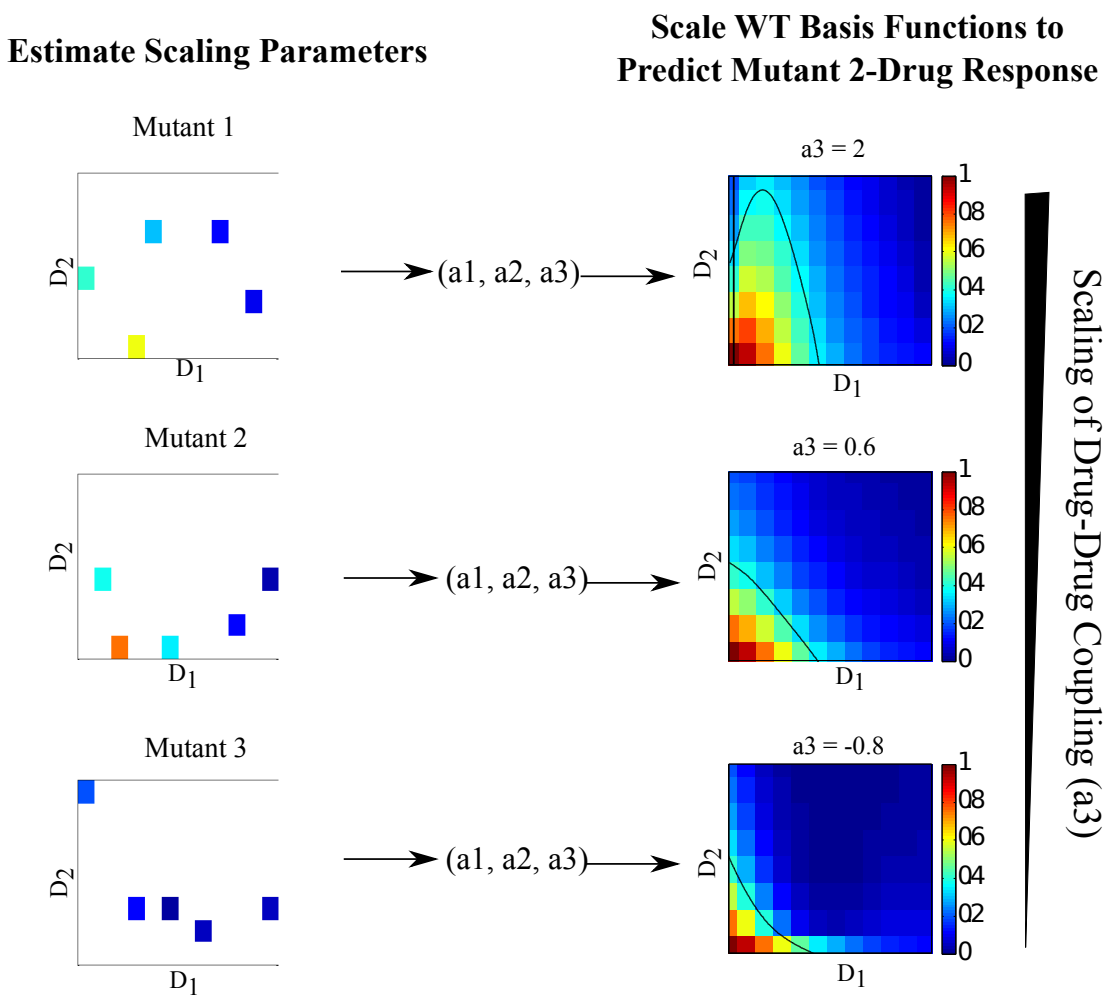
Estimate Scaling Parameters
Scale WT Basis Functions to
Predict Mutant 2-Drug Response
Mutant 1
Mutant 2
Mutant 3
D2
D1
(a1, a2, a3)
a3 = 2
a3 = 0.6
a3 = -0.8
1
08
06
04
02
0
Scaling of Drug-Drug Coupling (a3)

Figure 4

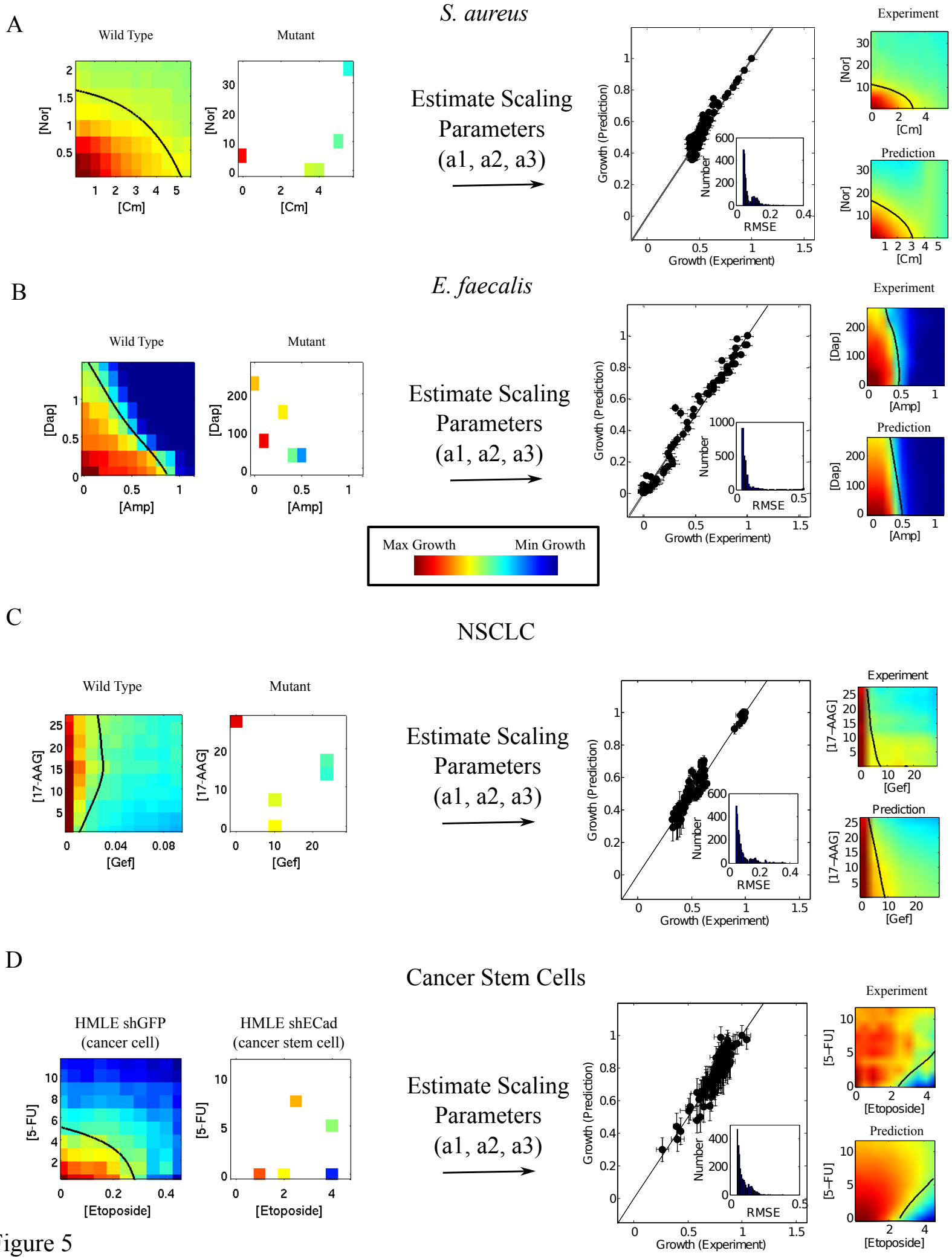
A
S. aureus
Wild Type
Mutant
[Nor]
[Cm]
Estimate Scaling Parameters (a1, a2, a3)
Growth (Prediction)
Growth (Experiment)
Number
RMSE
Experiment
Prediction
B
E. faecalis
[Dap]
[Amp]
Max Growth
Min Growth
C
NSCLC
[17-AAG]
[Gef]
D
Cancer Stem Cells
HMLE shGFP (cancer cell)
HMLE shECad (cancer stem cell)
[5-FU]
[Etoposide]

Figure 5

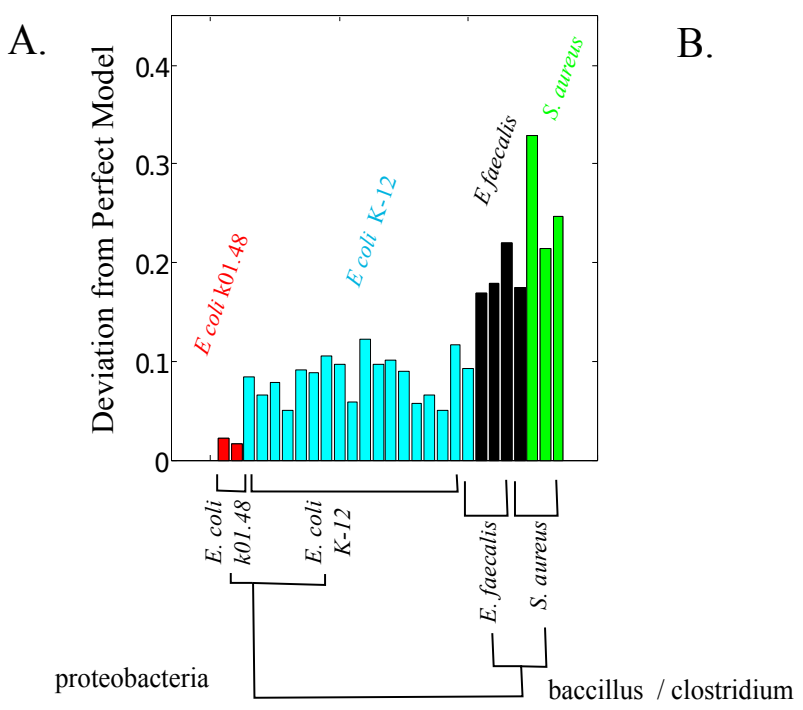
A.
Deviation from Perfect Model
0
0.1
0.2
0.3
0.4
E coli k01.48
E coli K-12
E faecalis
S. aureus
E. coli k01.48
E. coli K-12
E. faecalis
S. aureus
proteobacteria
baccillus / clostridium

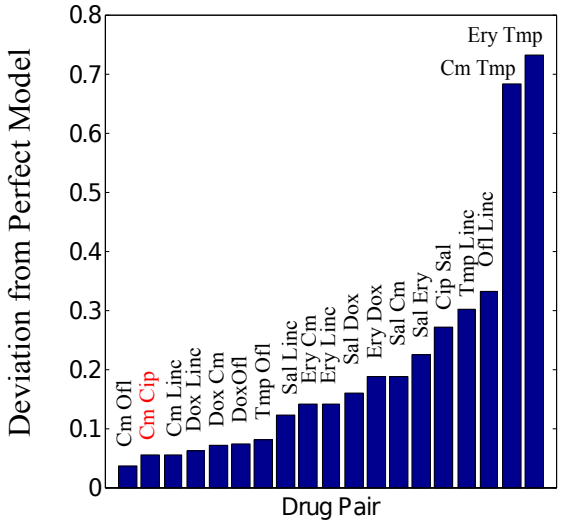
B.
Deviation from Perfect Model
0
0.1
0.2
0.3
0.4
0.5
0.6
0.7
0.8
Cm Ofl
Cm Cip
Cm Linc
Dox Linc
Dox Cm
DoxOfl
Tmp Ofl
Sal Linc
Ery Cm
Ery Linc
Sal Dox
Ery Dox
Sal Cm
Sal Ery
Cip Sal
Tmp Linc
Ofl Linc
Cm Tmp
Ery Tmp
Drug Pair

Figure 6